The Mechanism of Silicon Modification in Aluminum-Silicon Alloys: Impurity Induced Twinning

SHU-ZU LU and A. HELLAWELL

Modification of silicon by sodium in aluminum silicon eutectic alloy has been examined in detail by optical, SEM, and TEM methods. The aluminum phase is not significantly affected but the silicon becomes very heavily twinned. Modification by quenching does not involve an increase in twin density. Consideration of the atomic positions which attend the formation of growth twins on {111} planes suggests that adsorbed impurity atoms of suitable size, on the solid-liquid interface, could be responsible for changing the {111} stacking sequence, so promoting 'impurity induced twinning'; the optimum hard sphere radius ratio would be ≈ 1.65. It is proposed that this condition could be the first and principal requirement for a modifying agent to be effective in this system. It is shown further, that other reputed modifiers do also induce a higher twin density. Variations in the efficiency of individual elements to promote such an effect are discussed in terms of other relevant factors which include melting points and vapor pressures, the free energies of formation of compounds — notably of oxides, and the forms of alloy phase diagrams.

I. INTRODUCTION

In eutectic systems where one phase solidifies in a faceted manner and the other(s) nonfaceted,[1,2] it is well known that the eutectic microstructures may change markedly with solidification conditions (cooling/growth rates) and also with minor additions of certain specific modifying agents. Apart from the complex structures of cast irons, the earliest example of this type of behavior was reported for the Al-Si system some 65 years ago, following an accidental introduction of sodium fluoride to a flux.[3] Since then, the problem of 'modification' in this system has been the subject of several hundred publications in the literature and a number of reviews (*e.g.*, References 4 and 5).

While there appear to be a variety of structural changes,[6] that which has received the most attention is the one where the minor silicon phase is modified from a flake to a fibrous morphology; this can be accomplished without specific modifying additions at rapid cooling rates, with equivalent growth rates $\gtrsim 1$ mm s^{-1} — sometimes termed 'quench modified' — or at much slower rates by minor additions of sodium ($\cong 0.01$ wt pct), strontium ($\cong 0.1$ wt pct) and less certainly, with other alkali, alkaline earth, and rare earth metals.[4]

There have been various suggestions as to how the impurity additions cause modification to occur, based on changes in phase equilibria or differing nucleation or growth kinetics for the minor silicon phase. In this paper it is assumed that the mechanism is primarily concerned with the growth of the silicon phase, for the following reasons:

(a) Thermal analysis of impurity modified alloys shows depression of the eutectic and primary silicon arrests on cooling (by 5 to 10 K) but no such depression of the heating arrest for the former. Both the initial nucleation and horizontal parts of the eutectic cooling arrests are depressed; *i.e.*, there is no recalescence to raise the growth temperature toward that of the eutectic isotherm. There is no significant effect upon the freezing point of the aluminum phase.[7]

(b) The impurity (sodium, strontium, *etc.*) modified fibers are heavily twinned and are actually microfaceted, in contrast to the quench modified silicon which is essentially twin free and nonfaceted.[8,9] This observation confirms an earlier report of twin formation in silicon, grown epitaxially from aluminum solutions in the presence of sodium.[10]

(c) Sodium activity in an aluminum melt is sharply reduced by addition of silicon,[11] and scanning Auger spectroscopy indicates that sodium in a modified alloy is definitely associated with the silicon phase rather than in the aluminum matrix.[12]

In the following, we summarize what may be said of the two eutectic phases, primarily on a basis of scanning and transmission electron microscopy and selected area diffraction; some of this work has been reported elsewhere;[8,13] the principal internal feature of the silicon phase is that sodium and other specific impurity additions induce a high and variable density of growth twins which are not found in the pure binary alloy under any growth conditions.

II. EXPERIMENTAL

A master alloy of Al-12.6 pct Si was prepared from Al containing <60 ppm and Si containing <1 ppm of total impurities. The components were melted together in recrystallized alumina under argon and chill cast into cylinders 16 mm diameter and 80 mm long. Normal and modified samples were then prepared as follows.

Apart from some furnace cooled and directionally solidified material, the samples were prepared as 3 mm diameter cylinders from which TEM specimens could be cut directly for dishing and thinning. The alloy was therefore remelted under argon to a superheat of ~200 K and drawn into preheated quartz tubes of 3 mm bore. These samples were then allowed to slow cool to yield faceted flake structures or quenched directly into water to yield very fine fibrous eutectic (quench-modified). Modified samples were made in the same way, without the water quench, immediately after

SHU-ZU LU, formerly Visiting Scholar at Michigan Technological University, is Instructor, Department of Foundry Technology, Beijing University of Iron and Steel Technology, Beijing, People's Republic of China. A. HELLAWELL is Professor, Department of Metallurgical Engineering, Michigan Technological University, Houghton, MI 49931.

Manuscript submitted December 8, 1986.

addition of 0.05 to 0.07 wt pct sodium to the melt or larger additions of other modifying elements; see Section V–C.

For TEM examination the 3 mm diameter rods were sectioned on a slow speed, diamond wafer saw to slices ~0.25 mm thickness. These were then glued to a glass disk and hand polished down to ~0.1 mm; the samples were then ready for electrolytic or ion beam thinning. For the former, a Struers-Tenupol instrument was used with an electrolyte of 15 pct perchloric acid and 85 pct ethanol at 288 to 293 K. Perforated foils gave adequate thin areas for study of the eutectic silicon, the aluminum phase being preferentially removed.

Such specimens were examined in a Philips 301 instrument with 100 kV. In order to observe closely spaced twins it is necessary that the twin plane makes only a small angle with the electron beam. Therefore, it was necessary to use a tilting stage with ±45 deg about X and Y coordinates and to rotate carefully about various axes to ensure that twins were not overlooked; this was the most time-consuming aspect of the study. If a sample is tilted so that many parallel twins lie at a large angle to the beam — most obviously if they are at right angles to the beam — the superimposed twins are not resolved. Generally, only a single twin system, *i.e.*, on one (111) plane, will be visible, except in a single position — ⟨110⟩ close to beam axis — when two nonparallel {111} systems may be seen.

Bright- and dark-field images were observed and the corresponding SAD patterns obtained and indexed. Average twin spacings were obtained by the intercept method on micrographs.

About thirty satisfactory specimens were obtained from some sixty foils and the observations relate to more than one hundred selected areas.

Unmodified silicon flakes formed at slower growth rates are too thick for satisfactory TEM studies at 100 kV and for comparative measurements of twin contents, such samples were examined optically in a Zeiss Axiomat instrument using Nomarski contrast after etching (aqueous solution of 1 part HCl (48 pct), 2 parts HNO_3 (70 pct), 13 parts CH_3COOH).

Samples for SEM examination were deeply etched in 1 pct aqueous HCl for several days to remove the aluminum matrix. The surfaces were then carefully rinsed in distilled water, then in acetone, and then dried.[6]

III. THE SILICON PHASE

A. *Normal Flake*

This is found across a range of growth rates from ≈5 μm s^{-1} to ≈1 mm s^{-1},[6] but in the upper part of the range the flake habit is less distinct and more convoluted. The spacings and dimensions of the coarser flakes are also sensitive to the prevailing temperature gradient at the growth front,[6,14] so that it is misleading to make direct comparison between, *e.g.*, furnace cooled or cast samples and those grown unidirectionally at the same nominal rates;[15] the ingots typically have much lower prevailing temperature gradients than the latter and therefore coarser eutectic structures. Some measurements to demonstrate this point are to be found in Appendix I.

Flakes have a {111} habit and contain a few growth twins (Figure 1). The average twin spacings, λ_T, are about 0.4 to

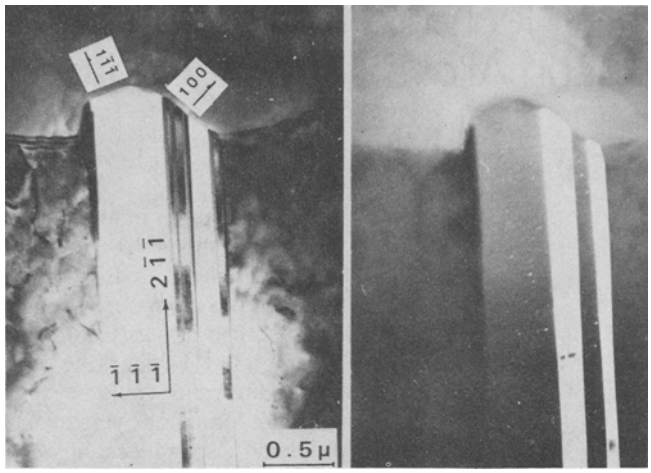

(*a*) (*b*)

Fig. 1 — Section through normal, faceted silicon flake with {111} habit and twins, TEM: (*a*) light field and (*b*) dark field.

1.0 μm in slowly cooled samples; this can be expressed as a twinning probability, $P = 2d/\lambda_T$, where d is the {111} interplanar spacing, here giving a value, $P \cong 10^{-3}$. The emergence of the growth twins on the external edges of growing silicon flakes does not result in very pronounced reentrant edges or grooves, and on a semi-faceted silicon flake at higher growth rates it may be seen that twins actually emerge on the nonfaceted part of the crystal (Figure 2). Given also the relatively wide spacing of the twins, it has been concluded[8] that the twin plane reentrant edge mechanism,[16,17] TPRE, is probably not important here for the kinetics of molecular attachment. However, an important consequence of such repeated twinning is that a single nucleation event can lead to a wide range of orientation changes during continuous growth of the silicon phase.[6,18]

Two branching modes may be identified: (i) large angle branching which is associated with twinning events and therefore at 70° 32′ to each {111} plane habit (Figure 3), or (ii) a variety of small angle branching, splitting, or overlapping events which are the more common (Figures 4 and 5). It is thought that these events take place at positions where areas of the silicon flakes are exposed to the liquid

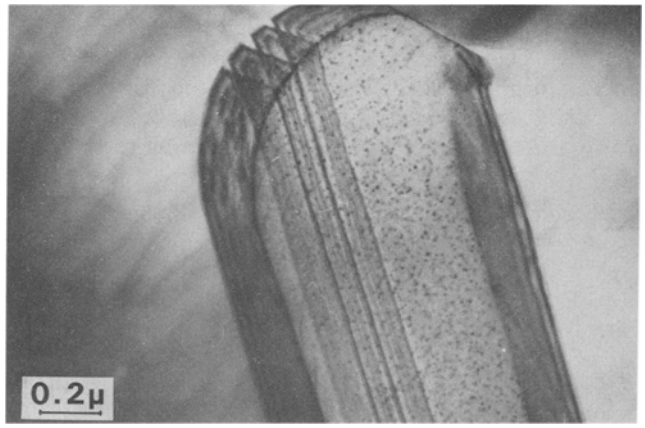

Fig. 2 — Semi-faceted growth tip of silicon flake, TEM twin crystal configurations out of contrast but twin interfaces visible. Note that twins emerge on nonfaceted part of tip

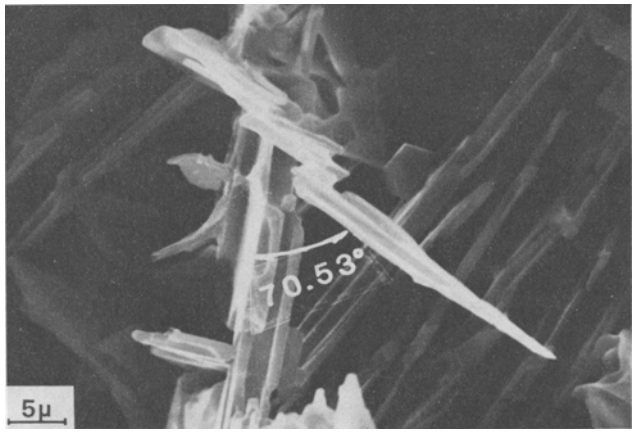

Fig. 3—Faceted silicon flakes after removal of metal matrix, showing large-angle branching, SEM.

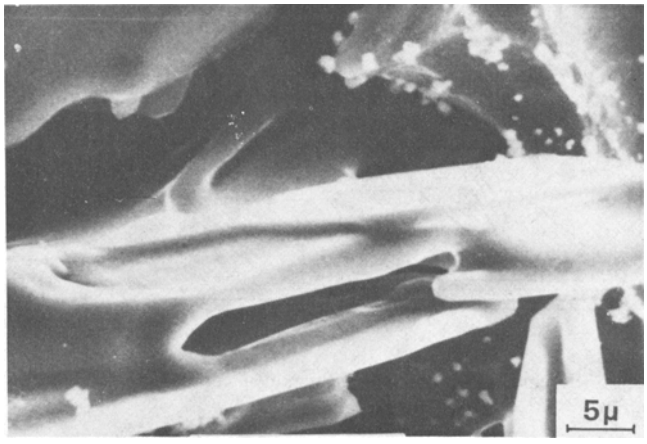

Fig. 5—Faceted silicon flakes after removal of metal matrix, showing branching in plane of a flake with subsequent overlap, SEM.

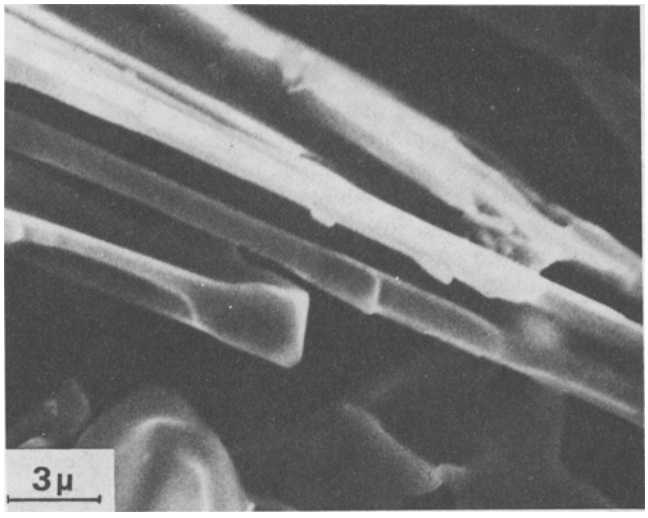

(*a*)

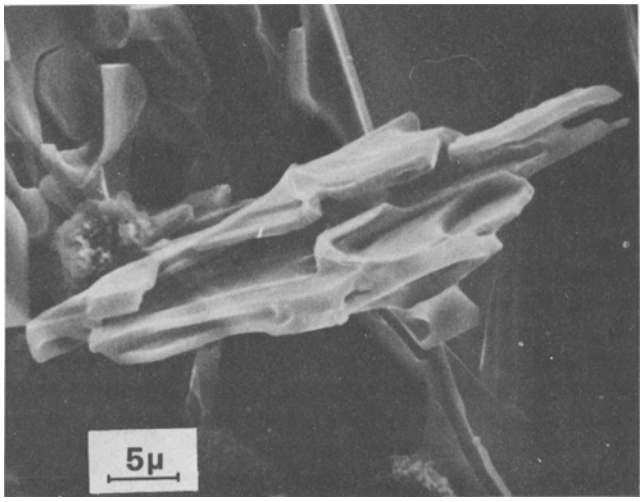

(*b*)

Fig. 4—Faceted silicon flakes after removal of metal matrix, showing small-angle splitting, SEM.

whenever the metallic matrix does not completely wet the sides of flakes; frequent ripple markings on these sides would seem to confirm this impression (Figure 6). Figure 7 summarizes the observed features schematically.

B. *Quench Modified Fibers*

These occur at growth rates $\gtrsim 1$ mm s^{-1}, and there is no evidence that they are sensitive to the temperature gradient. Fibers are quite smooth on external surfaces and are more often twin-free than otherwise (see Figure 8), so that it is not meaningful to discuss a twin density. The transition in shape would seem to correspond to a gradual change from somewhat anisotropic growth of flakes to entirely isotropic growth by an intrinsic mechanism at higher undercoolings.[19] The quenched fibers are, of course, very much finer than the slowly grown flakes and are also finer than the impurity modified fibers which form at relatively low growth rates.[8]

C. *Impurity Modified Fibers (Na and Sr)*

These occur across the range of growth rates which include flake morphologies in the pure alloy, but grow at a

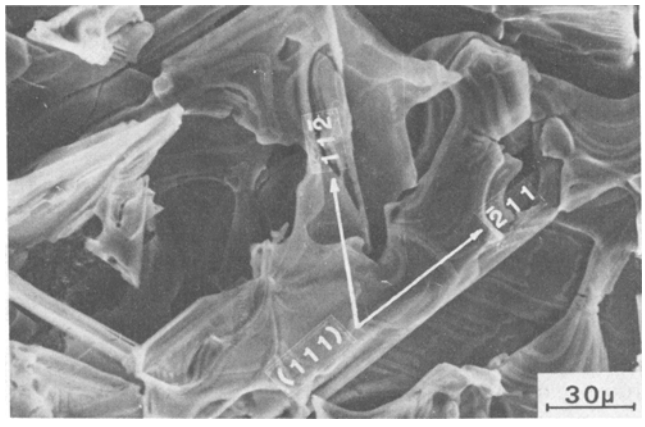

Fig. 6—Faceted silicon flakes after removal of metal matrix, showing ripple markings attributed to irregular wetting by metallic phase during growth, SEM.

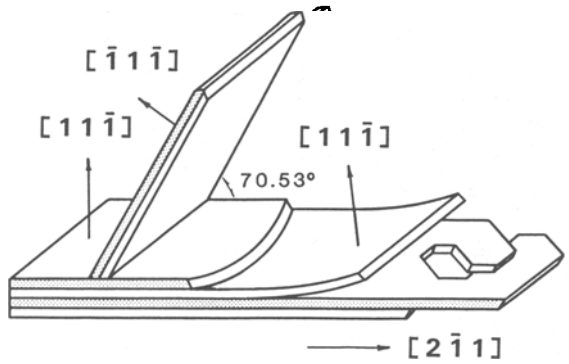

Fig. 7 — Schematic summary of branching in silicon flake (Figs. 3 to 6), with twin configurations shaded.

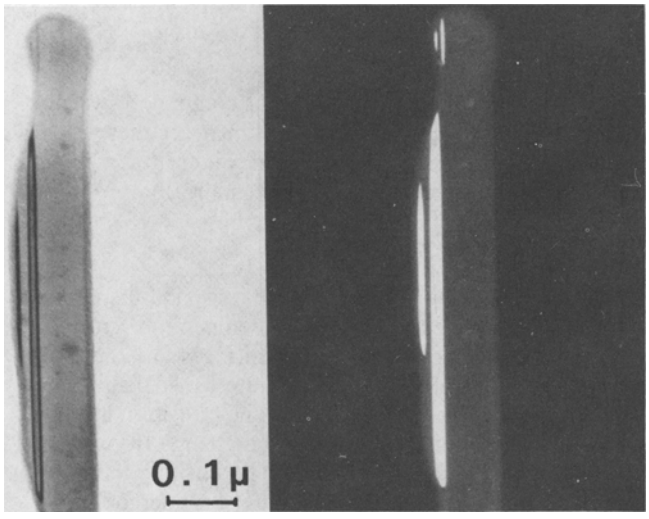

(*a*) (*b*)

Fig. 8 — Quench modified silicon fiber with smooth surface and rare example of twinning, TEM: (*a*) light field and (*b*) dark field

relatively isothermal front and are therefore not noticeably sensitive to temperature gradient. In directionally solidified samples at a given rate the phase spacing is only a little finer than the corresponding flake form.[15]

Detailed examination of the sodium modified fibers shows them to be externally rough or microfaceted and that they contain a very high twin density on up to four {111} systems (Figure 9); the preferred growth axis is then in a ⟨100⟩ direction, with symmetrical branching in ⟨211⟩ directions.[8,13] In some cases the mean twin spacing may be as low as 5 nm, and with reference to the prevailing growth rates this translates into as many as 10^4 twinning events per second. The structure is therefore remarkably imperfect crystallographically.

The external surfaces of these fibers are not smooth, as are the quenched fibers, but are rough or microfaceted on a scale determined by the twin density, and the general fibrous morphology is a consequence of growth in many directions on that fine scale. If it were possible to observe the silicon liquid growth interface, it would be expected that it must be multiply stepped and grooved as the numerous twins emerge, much as are the external surfaces.

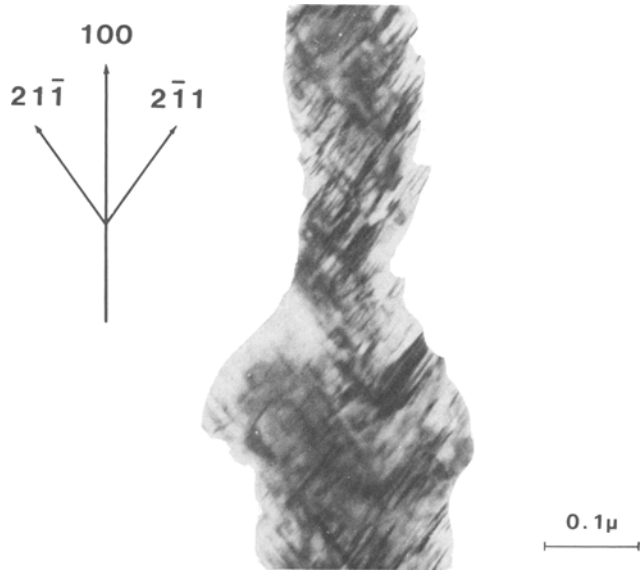

Fig. 9 — Sodium modified silicon fiber, aligned to reveal two {111} twinning systems, TEM. Note rough, microfaceted outline.

Similar TEM studies of strontium modified material[9,20] show a similar fibrous morphology although less heavily twinned or faceted for comparable analyzed levels of impurity concentration. If a sample is doped with sodium and quenched ("doubly modified"), the result is a fine fibrous structure with a very high multiple twin density, comparable with sodium modification at slower growth rates (Figure 10); that is, the promotion of twinning by impurity is independent of the growth conditions.

With regard to the location of the sodium in a modified alloy, it has been possible to establish by scanning Auger microscopy/spectroscopy[12,20] that the sodium is associated with the silicon phase, as would be implied from the preceding. The limits of resolution are not low enough to give further detail, such as how sodium is distributed within silicon fibers, but the technique can distinguish, within a lower limit of surface analysis of $\lesssim$0.5 pct, that there is no sodium in features such as primary aluminum dendrites.

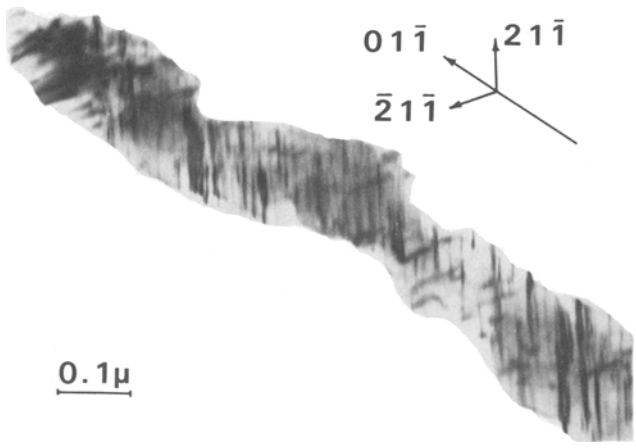

Fig. 10 — Doubly modified silicon fiber, quench and sodium modified, showing very high twin density and preferred ⟨011⟩ growth axis, TEM.

A natural conclusion from these observations would be that sodium (or strontium, *etc.*) is preferentially absorbed upon the silicon liquid front and thereby promotes frequent twinning. This is not to say, *a priori*, that twins are then a necessary feature to allow the kinetics of molecular attachment to operate, although the remarkably high twin density might reasonably be expected to play a significant part in providing step sources. The observation that the modified fibers do select a highly preferred ⟨100⟩ axis would support the importance of this kinetic mechanism, because this is the growth direction which incorporates the maximum, four, mutually oriented twin systems. This information is summarized in Table III; see later.

The consequence of this multiple twinning appears to allow anisotropic growth of silicon in so many directions simultaneously, that the morphology appears to be almost isotropic until resolved in detail.

IV. THE ALUMINUM PHASE

A. *Structure*

This is the major nonfaceted phase, containing ~1.65 wt pct Si at the eutectic temperature. As noted above, the aluminum liquidus arrests are not sensitive to minor sodium additions[7] and are only slightly depressed by strontium in accordance with the phase diagram.[21]

X-ray diffraction of strips, cut along the growth axis of directionally frozen samples, shows no preferred orientation for aluminum around flake or fibrous silicon.[6,22,38] Etching contrast in this and in other faceted/nonfaceted alloys (*e.g.*, Al-Al_3Fe/Al-Al_6Fe[23]) shows that the matrix continually changes orientation in bands along the growth direction. Closer examination by TEM, Figures 11(a) and (b), shows that in the unmodified alloy, the aluminum phase is comprised of many small subgrains on a scale of $\cong 1$ μm, having local misorientations of $\lesssim 2$ deg. These local variations in orientation can be followed by selected area diffraction patterns using Kikuchi lines (*e.g.*, Reference 24). Between the unmodified flake silicon the shapes of subgrains are variable and orientation changes haphazard; in the more closely coupled growth of the modified alloy the subgrains tend to be elongated in the growth direction, without a strongly preferred growth texture (Figures 12(a) and (b)), but with rotations of $\pm < 2$ deg about the growth axis from subgrain to subgrain.

These observations are broadly in agreement with those of other recent publications.[36,37,38] Exactly how the subgrains develop is not entirely clear; it has been suggested (*e.g.*, Reference 37) that they are a result of repeated epitaxial nucleation events upon exposed faces of flake silicon. Rather than the occurrence of discrete nucleation events, it would seem more probable to us, that the metal growth is continuous but irregular, as is implied by numerous examples of quenched growth fronts (*e.g.*, Reference 7) or as observed in transparent analogues.[1] In the modified alloys, the duplex growth front is much more closely coupled and more nearly isothermal and it is then that the metallic phase grows with elongated or 'columnar' subgrains.

B. *Epitaxial Phase Orientations*

A number of epitaxially preferred orientations have been reported between the phases[25] but, given the repeated twinning of the silicon phase, especially on the fine scale of modified fibers, it is difficult to see how the metal matrix can repeatedly adjust to a new epitaxial orientation as fast as growth proceeds.

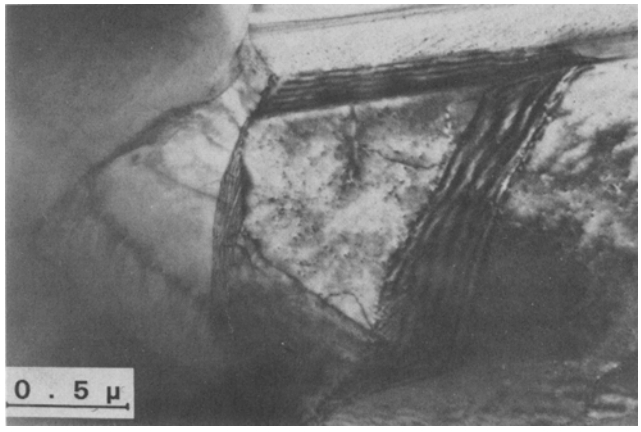

(*a*)

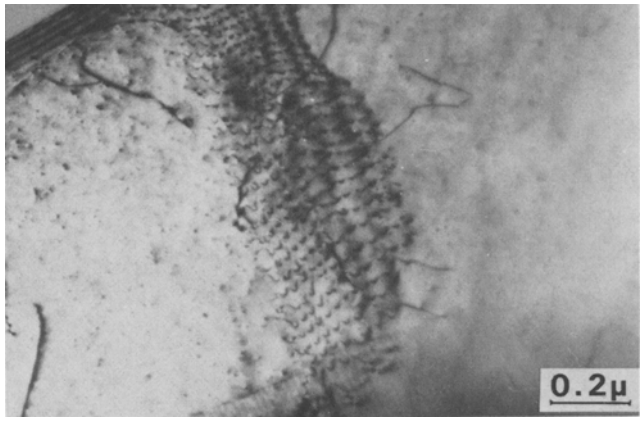

(*b*)

Fig. 11 — Structure of aluminum matrix in normal eutectic alloy, TEM, (*a*) showing silicon flake with adjacent subgrains and (*b*) detail of subgrain boundary

On a basis of >70 duplex SAD patterns, several very approximately preferred orientations might be identified for the normal structure (Table I). A typical example of the superposed 011 diffraction patterns is also shown in Figure 13. However, it should be noted that any one of the orientations could be described only within a ± 12 deg range. Given then the angular differences between the alternatives of Table I, it will be appreciated that on a projection these various configurations overlap to such an extent that specific preferences cannot be identified unambiguously

Table I. Some Possible Preferred Epitaxial Phase Orientations to Which Diffraction Patterns Approximate in the Normal Flake Structure

(i)	$(11\bar{1})_{Al} \parallel (100)_{Si}$, $[011]_{Al} \parallel [001]_{Si}$;
(ii)	$(100)_{Al} \parallel (\bar{1}1\bar{1})_{Si}$, $[011]_{Al} \parallel [011]_{Si}$;
(iii)	$(11\bar{1})_{Al} \parallel (11\bar{1})_{Si}$, $[011]_{Al} \parallel [011]_{Si}$;
(iv)	$(11\bar{1})_{Al} \parallel (11\bar{1})_{Si}$, $[011]_{Al} \parallel [112]_{Si}$;
(v)	$(01\bar{1})_{Al} \parallel (11\bar{1})_{Si}$, $[111]_{Al} \parallel [112]_{Si}$.

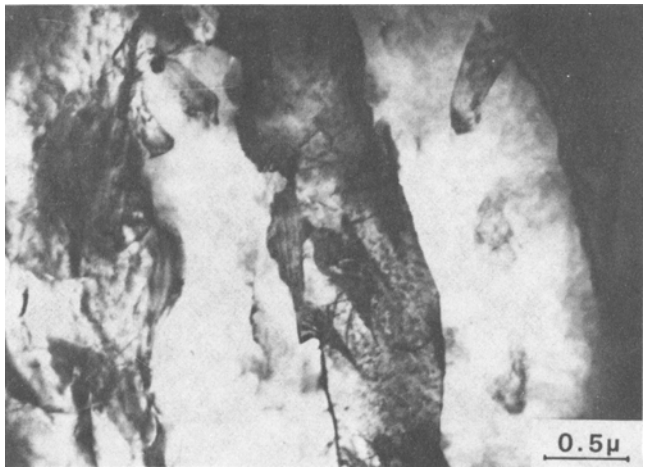

(*a*)

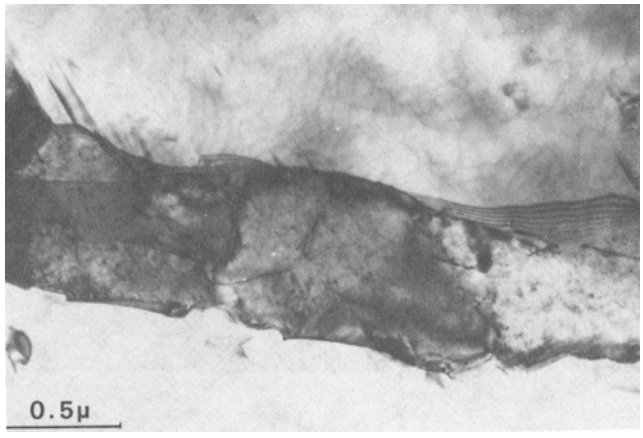

(*b*)

Fig. 12—Elongated aluminum subgrains which occur between sodium modified fibers, TEM

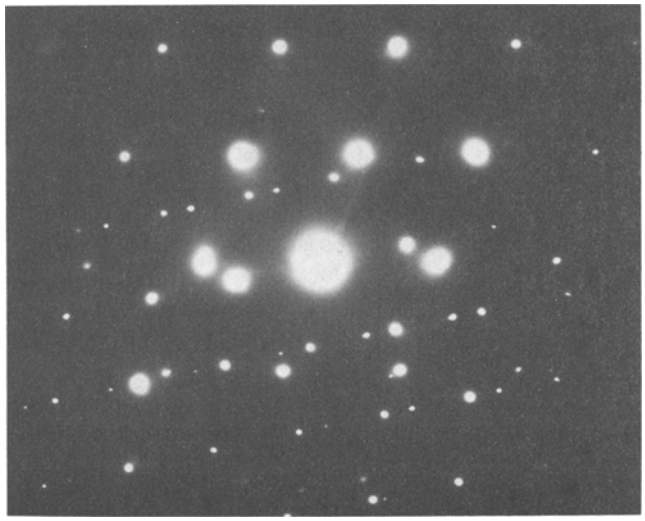

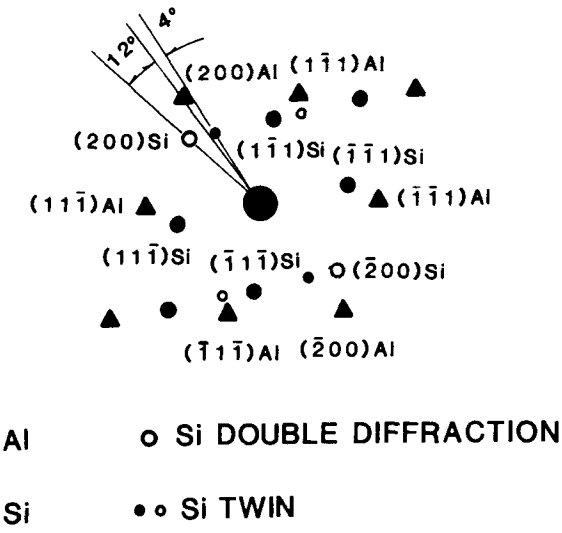

Fig. 13—Superimposed SAD patterns from adjacent aluminum and silicon phases, showing an approximately preferred epitaxial configuration: (100) Al‖(1̄1̄) Si, [011] Al‖[011] Si, with 4 deg and 12 deg deviations.

and it is probably futile to discuss the problem in terms of lattice or plane matching arguments.

In the fibrous, impurity modified alloy, there can be no question of the metallic phase matching the multiply twinned silicon and, indeed, no preferred expitaxial configurations can be detected.

Therefore, from the above, taken with the previously-mentioned absence of sodium in the aluminum phase, we conclude that the behavior of the metal is of minor importance to the mechanism of modification, except perhaps, with regard to its ability to dissolve or reject the modifying component. In this last respect, the case of sodium may be unique; see subsequent discussion. Any variations in the fine structure of the metallic phase may be regarded as a consequence of the silicon modification rather than an original cause of the effect.

V. DISCUSSION AND FURTHER RESULTS

A. *Identification of Modifying Elements—Atomic Radii*

Emphasis has been placed upon the incidence of twinning induced in silicon by sodium and strontium, which is accompanied by a morphological transition to microscopically rough fibrous shapes. In addition to these two modifying agents, the literature includes references to a range of other elements which have been reported, qualitatively, to promote a comparable shape change to a greater or lesser degree.[6,26–29] These other observations were based on optical microscopy and visual impressions of micrographs; only in the cases of sodium and strontium do we know for a fact that the shape change is also accompanied by twinning, of which it is a consequence. The other active elements are among the alkali, alkaline earth, and rare earth metals, and we note that these elements have in common, large atomic radii compared with silicon, as shaded in Figure 14.[35] These elements are listed in Table II in order of atomic radii, together with other properties which may be relevant to the general problem, including melting points, vapor pressures, and free energies of oxide formation, as available. It is noticeable also that the other properties cover very wide ranges. These will be discussed subsequently, but first we focus upon the

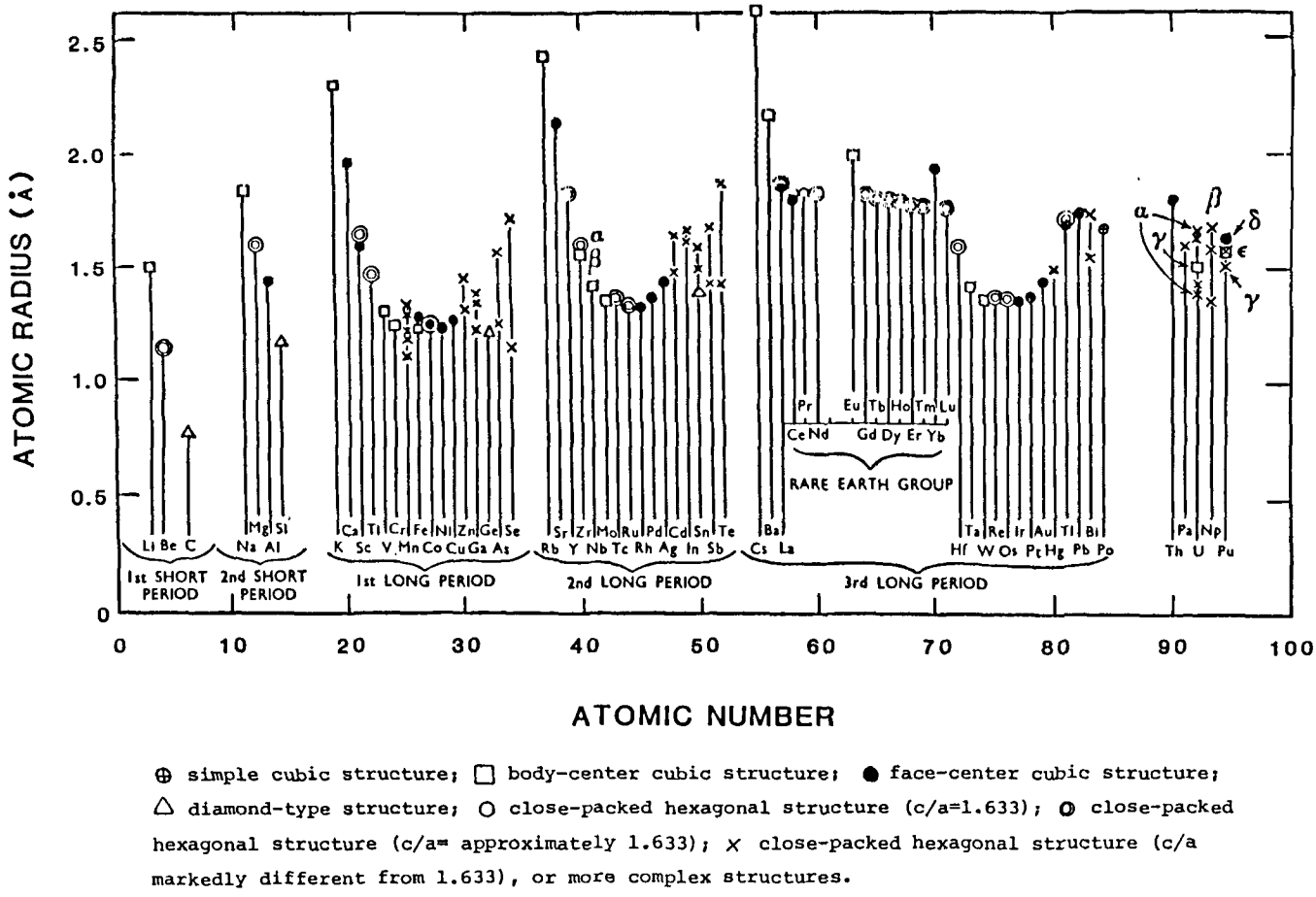

Fig. 14 — Plot of atomic radii *vs* atomic number (after Ref. 35), with range of radii which includes elements capable of producing silicon modification-shaded.

atomic radii and their possible relevance to the formation of growth twins.

B. *Impurity Induced Twinning*

We suppose, from the foregoing, that the modifying component is incorporated into the silicon by adsorption at the solid-liquid growth front. The modification is effective at growth rates where silicon normally grows anisotropically and therefore predominantly by extension of mono- or multi-step sources across the {111} closely packed planes. The modifier behaves as if these step sources were poisoned, as by accumulation of ad-atoms at such steps in sufficient density to create a "traffic problem", discussed in a general context by Cabrera *et al.*[30] Apparently, from thermal analysis data, the interfacial undercooling increases and the consequence is repeated twinning, as if step sources were temporarily halted. The critical concentration can be discussed in terms of a mean separation of ad-atoms below which a step is prevented, by line tension, from growing between them (somewhat similar to arguments used to discuss the pinning of dislocations by dispersed particles), shown schematically in Figure 15. The question then arises as to why, when a pinned step is reactivated or overgrown, the continued propagation should be in a twin configuration, *i.e.*, from -AABBCCAABBCC- to -AABBCCA ACCBBAA.

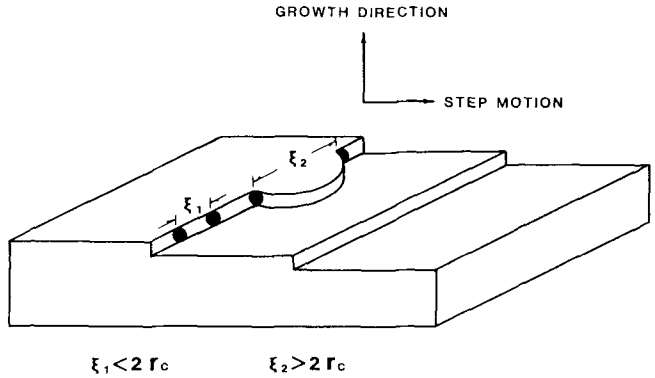

Fig. 15 — Schematic representation for adsorption of impurity atoms at monolayer steps on a growth interface (after Ref 30): ad-atom spacing $\zeta \gtrsim 2r_c$, where r_c is some critical dimension for layer extension.

One possible explanation for this effect can be envisaged by considering the detailed hard sphere geometry for the twin event, as in a 011 projection, Figure 16. It may be seen, that an impurity atom of appropriate size would force a monolayer step to miss one regular close packed position and so fall into the next alternative stacking sequence, thereby creating a twin. Geometrical calculation of the necessary hard sphere size, Appendix II, requires a specific radius ratio, r_i (modifier):r (silicon) = 1.646. This result, falling

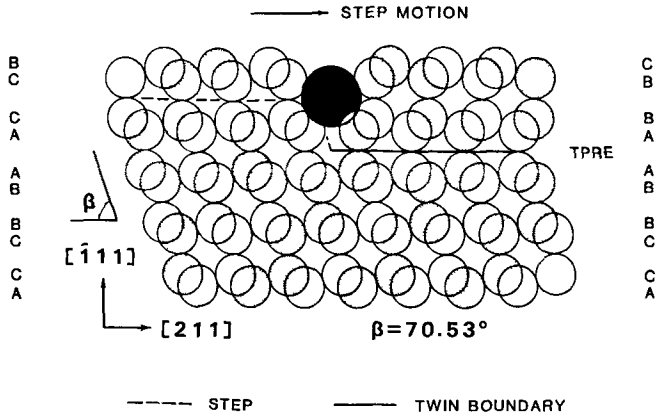

Fig. 16—011 plane projection of diamond cubic lattice to show how an impurity atom of certain size could promote twinning by causing a growth step to assume the alternative {111} stacking sequence, model for "impurity induced twinning"; see also Appendix II.

on Table II or Figure 14 between La and Yb, is based on the simpler face-centered cubic lattice rather than diamond cubic, but twinning in these two lattices is geometrically the same, *i.e.*, a 60 deg rotation about a {111} normal. The only geometric difference between the two is that the more open diamond cubic lattice might be expected to allow wider deviations from the hard sphere value than would the close packed structure. Therefore, it is suggested that this size factor could be the first and principal requirement for promotion of "impurity induced twinning", and by extension for modification of silicon in this (or any) system. The argument can be expected to apply only to crystal-liquid interfaces which are faceted, growing essentially by layer extension across close packed planes. Clearly, there are wide variations in the ability of elements around the 'correct' size ratio to effect twinning, and they are certainly dependent on factors other than just the size ratio. Before considering these other factors, it is in order to describe the incidence of twinning in some cases other than sodium and strontium for which the size ratios are comparable.

C. *Additions of Barium, Ytterbium, and Calcium*

Barium and calcium have been variously described as 'moderate' or 'weak' modifying agents (*e.g.*, Reference 26); there are no reports for additions of ytterbium. Additions of these metals were made to molten eutectic alloy in alumina crucibles, under argon at 900 to 1000 K, at an initial concentration of ~0.5 wt pct, after which the samples were furnace cooled at ~5 K minute; a mean growth rate of 20 μm s^{-1} to 50 μm s^{-1} would apply. Samples were then examined by optical and TEM methods, the latter being thinned by ion beam milling. It was previously established that chemical and ion beam thinning produced identical results in a given sample with sodium and with strontium additions.[8,9,20] The results are illustrated by Figures 17 through 19((a) through (c)), showing significant modification on an optical basis for Ba and Yb and a weak effect for Ca—the effects were somewhat uneven, especially close to external surfaces. On a basis of two or three successful thinning operations, all samples showed a significant rise in the silicon twin density by comparison with unmodified material; these results are summarized in Table III together with data for normal flake, quench, and sodium modified fibers (from Reference 8) and for strontium modified material (from Reference 9 and confirmed by us, Reference 20). It should be emphasized that the results for Sr, Ba, Yb, and Ca are much less exhaustive than for Na modified, quench modified, or normal silicon flake, but we consider them sufficient to make the point, namely, that

Table II. Possible Modifying Additions in Order of Atomic Radii

Element	At. Rad r (Å)	r/rsi	mp (K)	VP at 1000 K (atm.)	$-\Delta G$ Oxide (kJ/mol 1000 K)	$\frac{K}{[MO][Al]}{[Al_2O_3][M]}$	Effect
Cs	2.63	2.37	301	1.675	156		
Rb	2.44	2.08	311	1.451	185		
K	2.31	1.97	336	0.732	209		
Ba	2.18	1.85	998	$5 \cdot 10^{-5}$	482	20	x
Sr	2.16	1.84	1042	$1 \cdot 10^{-3}$	480	15	x
Eu	2.02	1.72	1095	$1.8 \cdot 10^{-4}$	~500		x
Ca	1.97	1.68	1112	$2.6 \cdot 10^{-4}$	509	$4 \cdot 10^{2}$	x
Yb r^*	1.93	1.65	1097	$5.6 \cdot 10^{-3}$	~500	$1.5 \cdot 10^{2}$	?
La	1.87	1.59	1193	10^{-6}	487		x
Na	1.86	1.58	371	0.2	367	$2.7 \cdot 10^{-5}$	xx
Ce	1.83	1.56	1071	10^{-16}	497		x
Pr	1.82	1.55	1204	10^{-13}	524		x
Nd	1.82	1.55	1283	10^{-11}	452		x
Sm	1.81	1.54	1345	10^{-5}	510		
Y	1.81	1.54	1796	10^{-15}	506		
Gd	1.79	1.52	1584	10^{-14}			
Tb	1.77	1.51	1633				
Mo	1.76	1.50	1743	10^{-10}			
Er	1.75	1.49	1795	10^{-11}			
Li	1.52	1.29	454	10^{-3}	560		
Al	1.4310	1.22	933	$5.3 \cdot 10^{-11}$	457	comparison	
Si	1.1755	1.00	1683	$8.9 \cdot 10^{-17}$	354		

x signifies reported modifying effect. The horizontal line corresponds to the hard sphere radius ratio for impurity induced twinning, r^*.

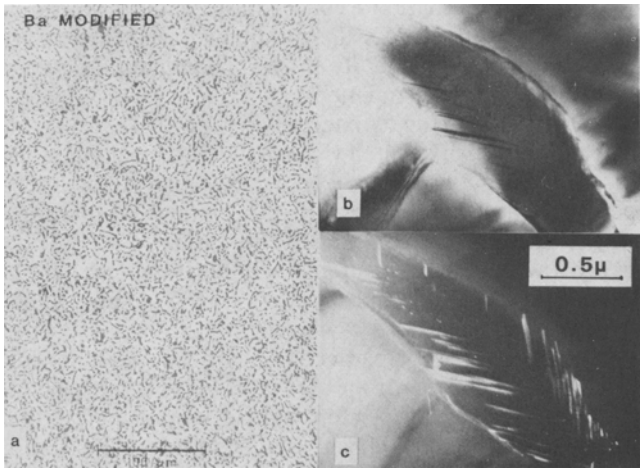

Fig. 17 — Microstructure of Al-Si eutectic alloy modified, respectively, by barium, ytterbium, and calcium: (*a*) optical, (*b*) TEM, bright field, and (*c*) TEM, dark field.

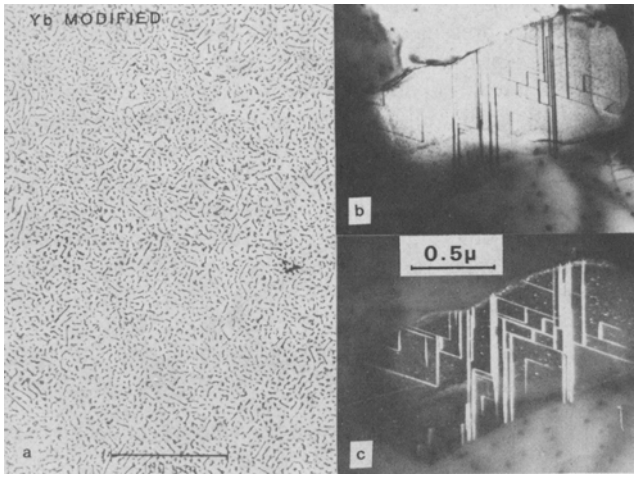

Fig. 18 — Microstructure of Al-Si eutectic alloy modified, respectively, by barium, ytterbium, and calcium. (*a*) optical, (*b*) TEM, bright field, and (*c*) TEM, dark field

shape change and twinning occur simultaneously. It then remains to discuss why the effects are variable, and, in particular, why sodium is so much more effective than other elements having atomic radii in the "favorable" size range.

D. *Other Modifying Factors*

As already noted, although the size factor might seem to be broadly applicable, there are, however, variations in effectiveness between elements of closely similar atomic radii (see Table II); for example, sodium is somewhat below the exact hard sphere ratio but is much more effective than either ytterbium or calcium which lie close to that of the geometrical model; barium and strontium have similar atomic sizes and effects.

Apart from the phase equilibria for the binary systems, Al-X and Si-X, which are somewhat idiosyncratic, the other factors which have been considered are the melting points and vapor pressures, and the free energies of oxide formation. Since modifying additions are made to aluminum-rich liquid, all comparisons relate to 1000 K and the oxide stabilities should be compared specifically with that of Al_2O_3 at that temperature. Some general comments for these other factors and for the three groups of additives are in order.

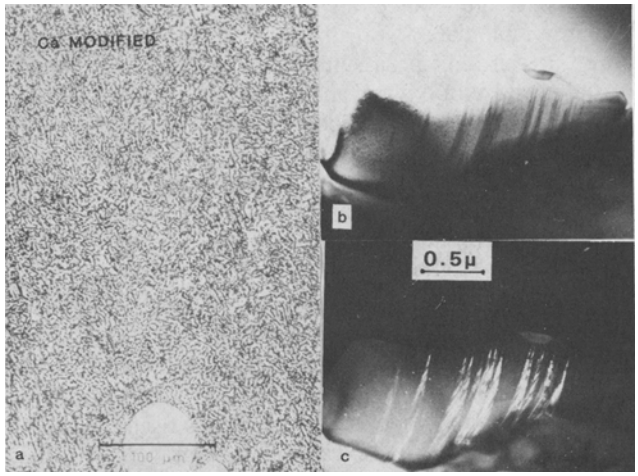

Fig. 19 — Microstructure of Al-Si eutectic alloy modified, respectively, by barium, ytterbium, and calcium: (*a*) optical, (*b*) TEM, bright field, and (*c*) TEM, dark field.

1. *Melting points and vapor pressures*

We expect that low melting point and high vapor pressure will make for rapid distribution throughout the melt. The alkalis clearly would be most effective in this respect; but, disregarding lithium, which is far below the effective size range (and is ineffective[31]), K, Rb, and Cs will boil off immediately and even sodium exhibits a notoriously rapid 'fade' in practice, with a vapor pressure of ~0.2 atmosphere at 1000 K. The alkaline earths have melting points close to the melt temperature but have relatively low vapor pressures; these should dissolve fairly quickly and be retained in solution for much longer times than the alkalis, which is presumably the advantage of using strontium in practice rather than sodium, even though its modifying effect is less dramatic. The rare earth metals have similar melting points and so will dissolve at about the same rates as the alkaline earths, but will also be retained for long times on the account of vapor pressures alone.

2. *Compound formation*

The oxidation of an addition will be rapid for all those elements with higher free energies of formation than aluminum, and we suppose that in the combined form the modifier will no longer be effective unless that had an equally strong affinity for silicon. We note that the alkalis will not be expected to oxidize as long as they remain in solution. Some *relative* estimates of the concentrations of free modifier in solution might be made for reactions of the form:

$$x\mathrm{Al_2O_3} + y\mathrm{M} \rightleftarrows 2x\mathrm{Al} + 3\mathrm{M}_x\mathrm{O}_y$$

$$e.g.,\ \mathrm{Al_2O_3} + 3\mathrm{Ca} \rightleftarrows 2\mathrm{Al} + 3\mathrm{CaO}$$

$$\text{giving } K = \frac{[\mathrm{Al}]^2[\mathrm{CaO}]^3}{[\mathrm{Al_2O_3}][\mathrm{Ca}]^3}$$

$$\text{where } \Delta G_{\mathrm{Al_2O_3}} - \Delta G_{\mathrm{CaO}} = -RT \ln K.$$

Values of K are included in Table II for those elements for which reliable data are available.[32,33] For comparative purposes, it can only be assumed that all relate to the same partial pressure of oxygen and to a large and constant reservoir of aluminum (and silicon): a large value of K corresponds to reduction of the melt by the third component and *vice versa*, *i.e.*, the additive tends to be in oxide form. We do not know if it is relevant, but we note also, that with respect to silicon, all the additives have more stable oxides, although only slightly so in the cases of the alkalis.

3. *Phase equilibria, Al-X and Si-X*

With the elements in question the aluminum phase diagrams fall into two categories, (a) those with extended liquid solubilities, low solid solubilities, and compound formation; these include the rare earths as far as are known and the alkaline earths excepting barium, and (b), those with negligible solid solubilities and wide liquid miscibility gaps, with monotectic points at very low concentrations; these include the alkalis, as far as are known, and barium. The relevance of the latter type of diagram has already been remarked, inasmuch as it offers a viable mechanism for an abrupt rise in modifier concentration at the solid-liquid growth front.

The silicon-X phase diagrams are generally incomplete as to detail, but in all cases there is at least one intermediate binary compound reported in the literature and in some cases ternary Al-Si-X compounds occur.[34] Thermodynamic data do not appear to be available for these compounds, but we consider that evidence of compound formation is an indicator that the additive will probably be strongly adsorbed at the silicon growth front, so that if the size factor is favorable, the possibility of promoting twinning is likely. We have already noted that sodium activity in molten aluminum is markedly reduced in the presence of silicon,[11] and it would be interesting to know how other additions are affected.

4. *Comparisons*

It will be obvious that discussions of all these factors can only be general and qualitative, at best, but it is possible to make some rational comments about the relative behavior of some additions. Referring to Table III, we confine our attempt to the three elements, sodium, strontium, and calcium, these being in decreasing order of modifying power. Calcium and sodium lie, respectively, at +2.5 pct and −2.5 pct of the geometrical size factor ratio, and strontium is somewhat above that ratio by ~12 pct. Sodium is rapidly dissolved but does not oxidize; it has a high vapor pressure and therefore evaporates easily and the effectiveness rises and fades quickly; the monotectic point at 0.01 wt pct Na means that the local liquid concentration at the growth front will rise abruptly across the miscibility gap. Observation reveals negligible solubility in solid aluminum; two intermediate silicides are reported.

Strontium will tend to oxidize fairly readily ($K \approx 15$) but much less so than calcium ($K \approx 4\ 10^2$); the melting points of both alkaline earths are comparable with the melt temperature, but the vapor pressure of strontium is ~four times that of calcium, although, relative to sodium, both are relatively low; the phase diagrams with aluminum are similar and do not contain liquid miscibility gaps; several similar silicides are reported.

We suggest that the particular activity of sodium is connected with the form of the Al-Na phase diagram, and the rapid solution and dispersion without oxidation. The low activity of calcium could be attributed to its rapid oxidation and low vapor pressure, while strontium is oxidized more slowly and maintains a higher vapor pressure, thereby retaining a longer but weaker modifying power than sodium.

Similar loose and rather inconclusive comments might be made about some of the others in Table III: barium is almost comparable with strontium in radius ratio, melting point, and free energy of oxide formation, but has a significantly lower vapor pressure; however, the binary Al-Ba diagram includes a liquid miscibility gap of limited range. On a basis of our somewhat superficial study it is a moderately efficient promoter of twinning, very similar to strontium. Data for ytterbium are incomplete, but it has a very stable oxide which we would expect to restrict its effectiveness (*e.g.*, Ca), but a relatively high vapor pressure; the Al-Yb diagram has not been determined but there are a number of silicides with this and other rare earth metals, so that all are probably surface active with silicon.

E. *A Criterion for Modifying Efficiency and Further Research*

The present work has shown that modification of flake silicon to an approximately fibrous morphology is attended by, and is probably a consequence of a high density of growth twins. The density of these impurity induced twins varies considerably from one element to another and one criterion which might be used to express the relative modifying efficiency of an addition is the ratio of twinning probability — as in Table II — to the analyzed atomic percent of impurity *remaining in the silicon phase*. The conditions of addition would need to be rigorously controlled (temperature, time before solidification, and conditions thereof) for such a comparison to be worthwhile, and the principal difficulty remaining is that we do not presently

Table III. Measured Twin Spacings and Probabilities in Several Impurity Modified Systems

	Estimated Average Growth Rate, V (μm s^{-1})	Average Twin Spacing, λ_T (nm)	Twin Probability *P
Normal (flake)	25 to 100	400 to 1000	6×10^{-4} to 1×10^{-3}
Quench modified (fiber)	1000 to 2500	—	very small
Na modified (fiber)	25 to 100	5 to 12	0.05 to 0.06
Sr modified (fiber)	25 to 100	30 to 100	6×10^{-3} to 0.02
Ba modified (fiber)	25 to 100	30 to 100	6×10^{-3} to 0.02
Ca modified (fiber)	25 to 100	100 to 200	3×10^{-3} to 6×10^{-3}
Yb modified (fiber)	25 to 100	50 to 150	4×10^{-3} to 0.01

Twinning probability $P = 2d/\lambda_T$ where d = {111} interplanar spacing in silicon

have available a suitable analytical technique for the localized chemistry. An exhaustive study would entail an ambitious research program.

Probably a more promising approach to the problem would be to study the epitaxial growth of silicon from metallic solutions onto silicon substrates, as has already been demonstrated elsewhere.[10,18] If such experiments were conducted under measured partial pressures of impurities, with controlled growth rates, the probability of obtaining measurable comparative data should exceed that possible with bulk liquid samples and additions thereto.

Finally, silicon modification is not restricted to aluminum alloys and has been reported for the similar eutectic system, Ag-Si.[6] If, therefore, the modifying mechanism is indeed general for silicon, it should apply to other faceted diamond cubic phases such as germanium or III-V compounds, with appropriate allowances for atomic radii and for the relevant factors which have been discussed here. The argument is probably relevant only to materials which solidify in a faceted manner, by extension of monolayer or multilayer steps, and would not be expected to apply to metals where growth is essentially isotropic and not significantly dependent on crystal defects.

VI. SUMMARY AND CONCLUSIONS

1. The addition of elements to molten alloys containing silicon can promote a transition in the morphology of the silicon phase by inducing growth twins. The metal matrix in Al-Si alloys is not affected significantly by such additions.
2. The modifying elements include a number of alkali, alkaline earth, and rare earth metals, all of which have significantly larger atoms than silicon and also form a range of silicides. In a modified alloy these impurities are associated with the silicon phase and it is concluded that they are adsorbed upon the silicon liquid growth front.
3. Assuming such surface adsorption of impurity atoms, a simple hard sphere model for atomic positions on {111} close packed planes of the silicon suggests that sufficiently large ad-atoms could promote twinning by displacing a {111} monolayer growth step to the alternative stacking sequence; geometrically the ideal radius ratio r modifier:r silicon, would be 1.646.
4. It is suggested that such a simple size factor requirement is a first condition for an impurity to cause structural modification in this and other systems containing silicon. The term "impurity induced twinning" has been used.
5. It is noted that other elements having atomic radii in the "favorable" range, including strontium, barium, ytterbium, and calcium, exert a similar but weaker effect than sodium with coincident shape change and twin formation.
6. An attempt has been made to discuss individual modifying effects on a rational basis. The complicating factors which have been considered are the melting points and vapor pressures, free energies of formation of oxides, and the forms of binary phase diagrams of the type Al-X and Si-X.
7. Although precise and detailed observations are limited, it is noted that silicon modification is not restricted only to the Al-Si system and it is suggested that the effect may apply more widely to other diamond cubic phases such as germanium and III-V compounds.

APPENDIX I

The influence of temperature gradient on silicon flake spacings

The point to be explained here concerns inter-flake spacings of silicon in ingots or castings *vs* directionally solidified samples grown at the same or comparable rates. The object is to illustrate that because coarse flake spacings are sensitive to temperature gradient, the lower temperature gradients in the former can produce different phase spacings to the latter, even if the growth rates are similar. The average phase spacing, λ, is related to the growth rate, V, and temperature gradient, G, by a relationship of the form

$$\lambda^2 V = AG^m$$

where A and m are constants. On a basis of experimental observations,[14] the equation is:

$$\lambda^2 V \approx 2.5 \cdot 10^{-6} G^{-2/3} \text{mm}^3\ \text{s}^{-1}$$

or at given V but at two gradients, G_1 and G_2, we have $\lambda_1/\lambda_2 \approx (G_2/G_1)^{1/3}$. Comparing typical values of temperature gradients in castings, $G_1 \leqq 0.2$ K mm^{-1},[7] and in directionally solidified samples, with $G_2 \approx 5$ K mm^{-1}, we would obtain:

$$\lambda_1(\text{casting}) \approx 3\lambda_2(\text{directional})$$

This ratio agrees very well with comparisons made by Flood and Hunt[15] for $V = 6.7\ \mu$m s^{-1} of $\lambda_1 \approx 12\ \mu$m (castings) and $\lambda_2 \approx 4.5\ \mu$m (directional).

Direct comparisons between the two freezing conditions are not, therefore, comparable unless temperature gradients are also taken into account.

APPENDIX II

Calculation of the atomic radius ratio of the impurities to the matrix crystal required by the crystallographic geometry for the impurity induced twinning

Assume the matrix crystal has a fcc structure with an atomic radius of r and the atomic radius of the impurities is r_i. In order for a row of adsorbed impurity atoms to induce a {111} twin during the interaction of the impurity atoms with intrinsic steps on the {111} interface, the r_i/r ratio is required by a geometric hard sphere relationship, as shown in the figures attached, (a) and (b)

$$CA = CF + Fa = Eg + Fa = \sqrt{3}r + \sqrt{3}r\cos\beta$$
$$= \sqrt{3}r(1 + \cos\beta)$$

For the normal triangle ABC:

$$AB = (AC^2 + BC^2)^{1/2} = [3r^2(1 + \cos\beta)^2 + r^2]^{1/2}$$
$$= r(4 + 6\cos\beta + 3\cos^2\beta)^{1/2}$$

For the normal triangle ODE:

$$OE = (OD^2 - DE^2)^{1/2} = [r_i + r)^2 - r^2]$$
$$= (r_i^2 + 2r_i r)^{1/2}$$

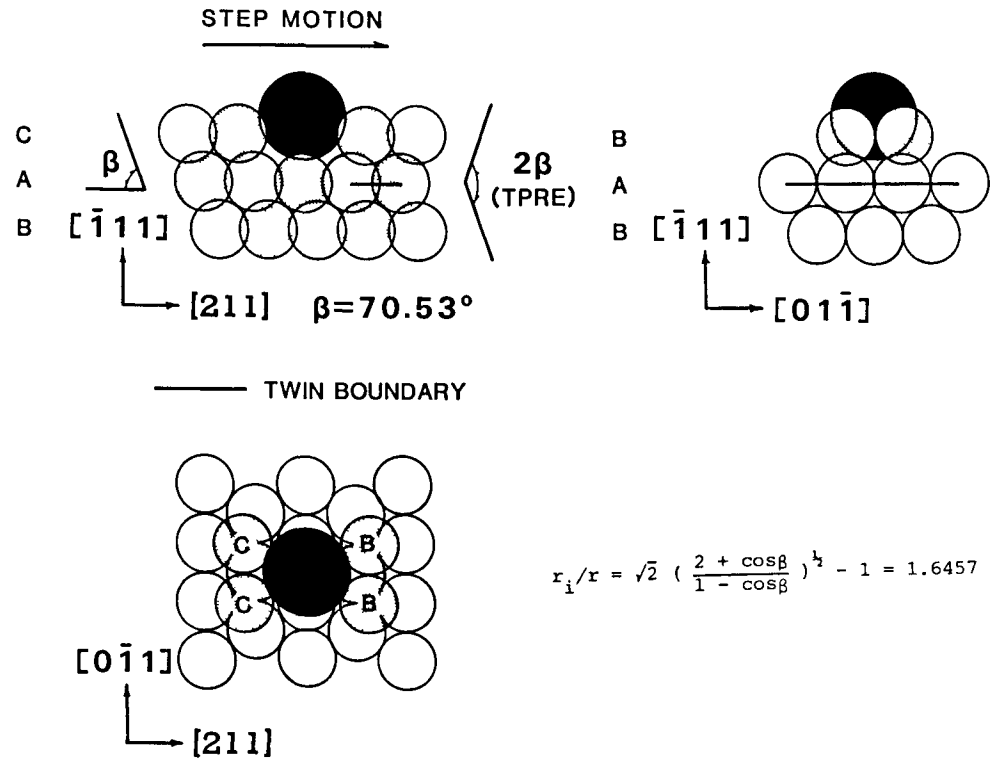

Fig. (a)—Various projections of the proposed model for twin formation, from the "side", 110, along the growth axis, 211, and from "above", 111.

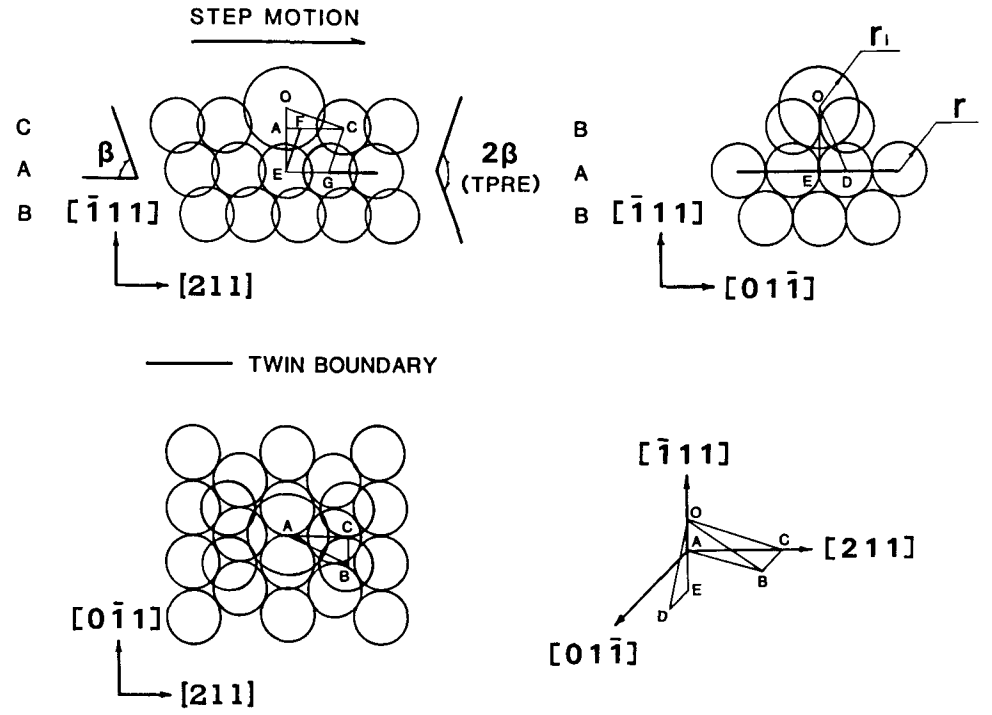

Fig. (b)—Corresponding geometrical constructions to calculate an ideal hard sphere radius ratio

And

$$OA = OE - AE$$
$$= (r_i^2 + 2r_i r)^{1/2} - \sqrt{3}\, r \sin\beta$$

Considering the normal triangle OAB:

$$OB^2 = OA^2 + AB^2$$

i.e.,

$$(r_t + r)^2 = [(r_t^2 + 2r_t r)^{1/2} - \sqrt{3}\, r \sin\beta]^2 + r^2(4 + 6\cos\beta + 3\cos^2\beta)$$

This yields an equation

$$r_t^2 + 2r_t r - \frac{3(1 + \cos\beta)^2}{\sin^2\beta} r^2 = 0$$

i.e.,

$$(r_t/r)^2 + 2(r_t/r) - \frac{3(1 + \cos\beta)^2}{\sin^2\beta} = 0$$

The solution to the above equation is:

$$r_t/r = \sqrt{2}\left(\frac{2 + \cos\beta}{1 - \cos\beta}\right)^{1/2} - 1$$

Provided $\beta = 70.53$ deg, the final result is then obtained:

$$r_t/r = 1.6457$$

The equivalent constructions for the diamond cubic lattice (see Figure 16 of text) are numerically the same but more difficult to draw.

ACKNOWLEDGMENT

This work was supported in part by the National Science Foundation, Grants #DMR 82-12115 and DMR 84-18845.

REFERENCES

1. J D Hunt and K. A. Jackson: *Trans TMS-AIME*, 1966, vol. 236, pp 843-52
2. R. Elliott: *Eutectic Solidification Processing*, Butterworths, London, 1983
3. A. Pacz: U.S. patent 1387900, 1920.
4. A. Hellawell· *Progr Materials Science*, 1970, vol. 15, p. 1.
5. G.K. Sigworth· *Trans A F S.*, 1983, vol. 91, pp 7-16.
6. M. D. Day and A. Hellawell. *Proc Roy Soc. A*, 1968, vol A305, pp. 473-91
7. M. D. Hanna, S. Z. Lu, and A Hellawell. *Metall. Trans. A*, 1984, vol. 15A, pp. 459-69.
8. S.Z Lu and A. Hellawell *J. Crystal Growth*, 1985, vol 73, pp. 316-28
9. M. Shamsuzzoha and L. M. Hogan: *J. Crystal Growth*, 1985, vol 72, pp 735-37.
10. V. de L. Davies and J. M. West: *J. Inst. Metals*, 1963-1964, vol. 92, pp. 175-80.
11. R. J. Brisley and D. J. Fray: *Metall. Trans. B*, 1983, vol. 14B, pp. 435-40.
12. S. P. Clough, M. B. Hintz, S. Z. Lu, and A. Hellawell: Michigan Technological University, unpublished work, 1986.
13. S. Z. Lu and A. Hellawell: *Aluminum Alloys—Their Physical and Mechanical Properties*, EMAS, London, 1986, vol. I, pp. 81-94.
14. B. Tolui and A. Hellawell: *Acta Metall.*, 1976, vol. 24, pp. 565-73.
15. S.C. Flood and J. D. Hunt: *Metal. Science*, 1981, vol. 15, pp. 287-94.
16. R. S. Wagner: *Acta Metall.*, 1960, vol. 8, pp. 57-60.
17. D. R. Hamilton and R. G. Seidenstricker: *J. Appl Phys.*, 1960, vol. 31, pp. 1165-68.
18. H. A. H. Steen and A. Hellawell: *Acta Metall.*, 1975, vol. 23, pp. 529-35.
19. K. A. Jackson: *Proc. 4th Int. Conf. on Crystal Growth*, North Holland, Amsterdam, 1974, p. 173.
20. S. Z. Lu: Ph.D. Thesis, Michigan Technological University, Houghton, MI, 1986.
21. M. D. Hanna and A. Hellawell: *Proc. Mat. Res Soc* , 1981, vol. 19, pp. 411-16.
22. M. Straumanis and N. Brakss: *Z. Phys. Chem. B*, 1937, vol. 38, pp. 140-55.
23. A. J. McLeod, L. M. Hogan, C. M. Adam, and D. C Jenkinson: *J. Crystal Growth*, 1973, vol. 19, pp. 301-309.
24. I.G. Davies and A. Hellawell: *Phil Mag.*, 1969, vol. 19, pp. 1285-97.
25. K. Kobayashi, P. M. Shingu, and R. Ozaki: *The Solidification and Casting of Metals*, The Metals Society, London, 1979, pp. 101-05.
26. C. B. Kim and R. W. Heine: *J. Inst. Metals*, 1963-1964, vol. 92, pp. 367-76.
27. Q. Zhang, S. Liu, and J. Hu. *Acta Met. Sinica*, 1984, vol. 20 (2), pp. 138-44.
28. Z. Y. Zhou, S. Y. Zhau, Z. R. Zhom, and Z. H. Yang: *Giesserei-Prax.*, 1983, vol. 4, pp 49-56.
29. Q. Y. Zhang, C. G. Zheng, and W. S. Han: *Acta Met Sinica*, 1981, vol. 17 (4), pp 130-32
30. N. Cabrera and D. A. Vermilyea: *Growth and Perfection of Crystals*, Wiley, New York, NY, 1958, p. 394.
31. M. D. Hanna and A Hellawell· *Metall Trans. A*, 1984, vol. 15A, pp. 595-97.
32. O. Kubaschewski and C. B. Alcock: *Metallurgical Thermochemistry*, Pergamon Press, Oxford, 1979
33. R R Hultgren: *Selected Values of Thermodynamical Properties of Metals and Alloys*, ASM, 1973
34. P. Villars and L. D. Calvert: *Pearson's Handbook of Crystallographic Data for Intermetallic Phases*, ASM, 1985, vols. II and III.
35. W Hume-Rothery and G. V. Raynor: *The Structure of Metals and Alloys*, The Institute of Metals, 1962, Part III, p. 65.
36. M. Shamsuzzoha and L. M Hogan: *J. Crystal Growth*, 1986, vol 76, pp. 429-39.
37. M. Shamsuzzoha and L M. Hogan. *Phil. Mag.*, 1986, vol. 54, pp 459-68.
38. L. M. Hogan and H. Song: *Acta Metall.*, 1987, vol 35, pp. 677-80